RESEARCH ON PIG BODY SIZE MEASUREMENT SYSTEM BASED ON STEREO VISION
/
基于立体视觉的猪只体尺测量系统研究

Yanli GENG*[1)], Xiaodong YUE[1)], Yankai JI[1)], Yanbo LIN[1)], Yanfang FU[2)], Shucai YANG[3)]
[1)]School of Artificial Intelligence, Hebei University of Technology, Tiajin, 300130 / China,
[2)]Hebei Provincial Animal Husbandry Station, Hebei 050035 / China,
[3)]Tianjin Mojieke Technology Development Co., Ltd, Tiajin, 300130 / China;
Tel: +8615320025316; E-mail: gengyl@hebut.edu.cn
DOI: https://doi.org/10.35633/inmateh-70-07

Keywords: *Pig body size measurement, KinectV2 camera, Point cloud, Calibration registration*

ABSTRACT
Body size of pigs is an important evaluation indicator in pig breeding. The traditional method of body size measurement is usually in manual way, which requires more employees and causes stress reactions of pigs. In response to the shortcomings of the traditional methods, this paper designed a system for measuring the body size of pigs based on stereo vision. The point cloud of both the calibration object and the pig was collected using dual KinectV2 cameras. Pre-processing was conducted using filtering and random sample consensus to remove background noise from the point clouds. As there was limited overlap between the two sides of the point clouds, the rotation matrix obtained from registering the calibration object was applied to the pig point clouds. Curve fitting and slicing were then utilized to measure the pig's body dimensions, including length, width, height, and abdominal circumference. The results of the study indicated that the mean absolute percentage error (MAPE) was 2.13% for body length, 1.02% for body width, 1.05% for body height, and 2.21% for abdominal girth. These results demonstrate the high accuracy and practical production value of the system.

摘要
生猪的体尺参数是生猪养殖情况的重要评判指标，传统的猪只体尺参数测量方式通常为直接接触式，需要消耗更多的人力并且易造成猪只的应激反应。针对传统体尺测量方法的缺陷，本文设计了一种基于立体视觉的猪只体尺自动测量系统。首先利用双 KinectV2 相机采集标定物与猪只的点云数据，利用滤波和随机采样一致性算法对采集的点云进行预处理，获取无背景的标定物与猪只点云；然后针对两侧点云重合度低的问题，将标定物配准输出的旋转矩阵应用于猪只点云配准；最后利用曲线拟合与切片处理方法测量猪只体长、体宽、体高和腹围。 试验结果表明，猪只体长测量平均相对误差为 2.13%，体宽测量平均相对误差为 1.02%，体高测量平均相对误差为 1.05%，腹围测量平均相对误差为 2.21%。该系统具有较高的估算准确性，在实际生产中有重要意义。

INTRODUCTION
The outbreak of African swine fever virus in 2018 has made a profound negative impact on pig farming industry (*Liu et al., 2020; Zhang et al., 2021*). The body size parameters are important indicator for evaluating the growth of pigs. In the traditional way, breeders measure the size with a tape measure. In this way, breeders keep close contact with the pig, which will increase the risk of disease in pigs *(Wang et al., 2018； Luo et al., 2018)*. The automatic measurement can effectively reduce the risk of disease in pigs, increase efficiency and accuracy of measurement and improve animal welfare *(Reinke et al., 2021; Cheng et al., 2021).*

In recent decades, two-dimensional cameras have been widely used in the field of computer vision *(Bewley et al., 2008; Chen et al., 2018; Junming et al., 2020)*. However, this technique has limitations in measuring animal body parameters, such as changes in light intensity, difficulty of background separation and image acquisition environment *(Viazzi et al., 2014).* With the development of machine vision and 3D point cloud processing technologies, these technologies are being used in the livestock industry *(He et al., 2020; Salau et al., 2014; Weber et al., 2014).* A visual image analysis system is designed by *White et al. (2005)*. The size and shape information of pig's back is obtained by a camera, which is used to monitor the growth of pigs. A noncontact weight estimation system for pigs is built by *Apirachhai et al. (2015)*. A camera is put on the top of the system, which is used to capture the image of pig's back. The body contour of the pig is extracted and the body length and profile length of the pigs is calculated.

The parameters of pig body size are used as inputs to the weight estimation model, and the MAPE in weight estimation is less than 3%. The interactive measurement software LSSA_CAU is designed by *Guo et al. (2017)* to estimate livestock body size based on point clouds. The point cloud of the pig is obtained by *Liu et al. (2014)* using a non-contact 3D scanner. The surface model of the pig is reconstructed to obtain the coordinates of the measurement points for each parameter. The thorax, surface area and volume of the pig are calculated. The top and side view depth maps of the pig are captured by *Pezzuolo et al. (2018)* using a Kinect depth camera. The coordinates associated with the pig's body parts are efficiently obtained from the point cloud reconstructed by the depth map, and then the body size parameters can be calculated. *Wang et al. (2018)* proposed a method for measuring pig body size based on a single-view point cloud. A complete point cloud of the pig's body is obtained using mirror imaging and body size parameters are measured. This method requires only one camera and reduces the complexity of image acquisition, but the measurement error is large. *Yin et al. (2019)* use the Kinect v2 to collect the local point clouds of pigs from the top, left and right angles simultaneously. The local point cloud is denoised by the neighbourhood curvature change method, and the complete pig body point cloud is obtained by registration. Finally, each body size is measured using an accurate estimation technique of multi-scale data. *Li et al. (2018)* propose a method for the construction of stereo vision. This method set up two cameras on the back to acquire images and automatically extract the body size measurement points of the pig.

In this paper, two KinectV2 cameras were placed symmetrically on the left and right sides of the measured object. The point clouds of calibration object and pigs were collected, which were denoised and segmented. The rotation-translation matrix of the point clouds was obtained by registering the calibration objects, which was used to register the pig point clouds. This method only needs to be calibrated once before collecting the point cloud, which can improve registration accuracy and speed. Finally, each body scale was measured by slicing and curve fitting, as shown in Fig 1.

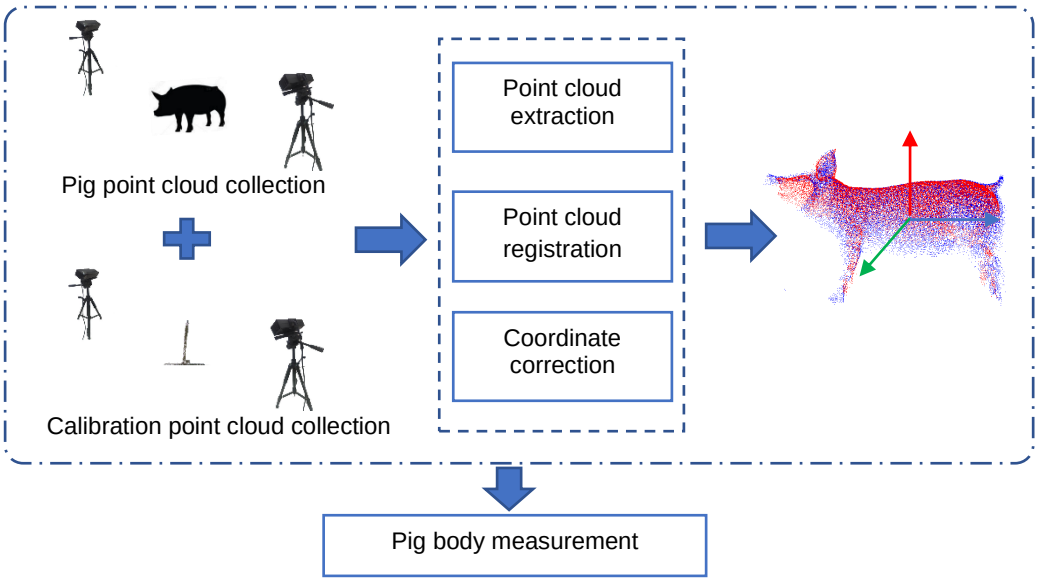

Fig. 1 - Technology Roadmap

MATERIALS AND METHODS

In this paper, a collection platform of point cloud was built in the laboratory. The Kinect cameras are placed symmetrically on both sides of the pig. The camera's height above ground level is 0.9 m. The horizontal distance between the two cameras is 1.2 m. The angle between the camera and the horizontal plane is 45° (as shown in Figure 2.a). The point cloud of pig on both left and right side are collected. The position of the camera must remain constant when collecting the point cloud of the calibration object and pig. In this way, the rotation matrix of the calibration object can be used in pig point cloud registration.

The measurement experiment platform was built in Dabei Farm, Cangzhou (as shown in Figure 2.b). Only one pig was allowed in the collection area. The location and placement of Kinect v2 cameras were same as that of the laboratory.

The breed of the pig is Yorkshire and the age ranged from 90-100 days. Data were collected from 9.30AM to 16.30PM. A total of 3510 point clouds were collected from 100 pigs in the experiment. All manual measurements of body size of pigs were measured by professional testers with tape measures. The measurement accuracy is 1 mm in the laboratory and 1 cm on the farm.

(a) **(b)**

Fig. 2 - Pig point cloud acquisition platform

Pig point cloud extraction

When acquiring point clouds of pigs, noisy points appear in the acquired point clouds due to the accuracy of Kinect v2, experimenter's operation, and environmental problems at the test site. In addition, there are discrete points far away from the main point cloud in the point cloud data due to the infrared diffraction problem and the influence of different surface textures of the measured object. In order to extract the pig point cloud and remove the noise, the following processes are applied to the point cloud.

1) Pass-through filter processing: Among the point clouds captured by Kinect v2, only some of them require subsequent processing. Therefore, with a clear target area, the point cloud is filtered by Pass-through, and the irrelevant point clouds can be quickly removed to obtain the point cloud of the pig area.

2) Statistical filter processing: Statistical analysis is conducted on the neighbourhood of each point in the point cloud obtained in step 1). Then all distances in the point cloud are assumed to form a Gaussian distribution, and its shape is determined by mean μ and standard deviation σ , Let the coordinate of the nth point in the point cloud be $P_n(X_n, Y_n, Z_n)$, The distance from this point to any point is S_i , as shown in Equation (1):

$$S_i = \sqrt{(X_n - X_m)^2 + (Y_n - Y_m)^2 + (Z_n - Z_m)^2} \quad (1)$$

Calculate the mean $\mu = \frac{1}{n}\sum_{i=1}^{n} S_i$ and standard deviation $\sigma = \sqrt{\frac{1}{n}\sum_{i=1}^{n}(S_i - \mu)^2}$ of the distance from each point to any point, when the average distance of a point close to k points is within the standard range $(\mu - x\sigma, \mu + x\sigma)$, the point is retained. If it is not within the standard range, it is defined as an outlier deletion.

3) Random sampling consistency split: Three points are randomly selected in the initial point cloud, and their corresponding plane equations are calculated $ax + by + cz + d = 0$. Calculate the algebraic distance d_i of all points to this plane, as shown in Equation (2):

$$d_i = \left| ax_i + by_i + cz_i + d \right| \quad (2)$$

Pick Threshold $d_{\max}$, if $d_i \le d_{\max}$, then the point is considered to be a point in the plane, otherwise it is an out-of-plane point. Repeat the above steps, setting the maximum number of iterations N and getting the surface with the most plane points. The normal vector n_z of the plane is calculated, and then delete it to achieve the effect of removing the plane. The effect of the point cloud after the above three steps is shown in Figure 3:

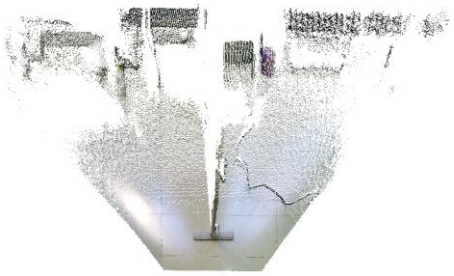

(a) Panoramic point cloud

(b) Point cloud extraction

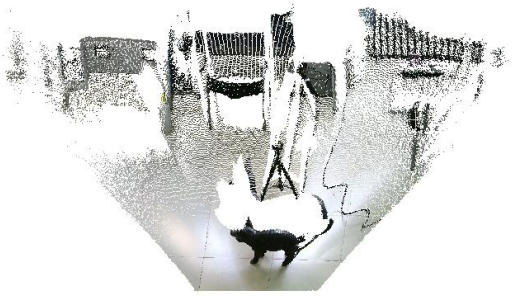

(c) Pig panoramic point cloud

(d) Pig point cloud extraction

Fig. 3 - Point cloud denoising segmentation processing

Calibration-based point cloud registration

The process of converting point clouds to the world coordinate system is called point cloud registration, and the stitching of point clouds is done by screening for overlap. In this paper, point clouds are captured horizontally symmetrically by the KinectV2 camera. The overlap of the pig point clouds is poor, resulting in low registration efficiency and accuracy. Therefore, fine and rough registration methods are designed to deal with the point clouds. The output translation and rotation matrix are used for the registration of the pig point clouds.

First, the calibration object is roughly registered. In the calibration of multiple depth cameras, the process is called rough registration, which involves obtaining the rotation and translation matrices of adjacent sub-regions and calculating the transformation into the same coordinates based on Equation (3).

$$\begin{bmatrix} x_1 \\ y_1 \\ z_1 \end{bmatrix} = R_{rough} \begin{bmatrix} x_2 \\ y_2 \\ z_2 \end{bmatrix} + T_{rough} = \begin{bmatrix} R_1 & R_2 & R_3 \\ R_4 & R_5 & R_6 \\ R_7 & R_8 & R_9 \end{bmatrix} \begin{bmatrix} x_2 \\ y_2 \\ z_2 \end{bmatrix} + \begin{bmatrix} t_x \\ t_x \\ t_x \end{bmatrix} \tag{3}$$

where:

R_{rough} is the space transformation matrix, T_{rough} is the translation vector.

The camera coordinate system of the right camera is set to the world coordinate system, and the point cloud acquired by the left camera is linearly transformed into the world coordinate system. Before the experiment, rotation and translation matrices were obtained by calibrating two KinectV2 cameras. The object is roughly registered by linearly transforming the left point cloud.

The right point cloud is used as the target point cloud, and the object to be registered is the linearly transformed left point cloud. Source point cloud S and target point cloud T are obtained, as shown in Equation (4).

$$\begin{cases} S = \{s_1, s_2, s_3, \cdots, s_n\} s_i \left(x_i, y_i, z_i\right)_{i=1,2,\cdots,n} \\ T = \{t_1, t_2, t_3, \cdots, t_n\} t_j \left(x_j, y_j, z_j\right)_{j=1,2,\cdots,n} \end{cases} \tag{4}$$

Improved ICP is designed for the fine registration of the origin point cloud S and target point cloud T and has a high retrieval speed.

The algorithm steps are as follows:

Step 1: The source point cloud and the target point cloud are inputted, and an Octree bounding box is established.

Step 2: The overlapping areas of the source point cloud *S* and the target point cloud *T* are searched for by Octree.

Step 3: Point clouds of overlapping regions are extracted and the corresponding point S' and T' are calculated, as shown in Equation (5).

$$\begin{cases} S' = \{s_1', s_2', s_3', \cdots, s_n'\}\, s_i'\left(x_i, y_i, z_i\right)_{i=1,2,\cdots,n} \\ T' = \{t_1', t_2', t_3', \cdots, t_n'\}\, t_j'\left(x_j, y_j, z_j\right)_{j=1,2,\cdots,n} \end{cases} \quad (5)$$

The original point cloud normal vector is calculated, and the normal vector angle threshold of the target point cloud is set to be larger than s_i'. The non-standard point cloud is deleted and two groups of corresponding points are obtained, as shown in Equation (6).

$$\begin{cases} S'' = \{s_1'', s_2'', s_3'', \cdots, s_n''\}\, s_i''\left(x_i, y_i, z_i\right)_{i=1,2,\cdots,n} \\ T' = \{t_1', t_2', t_3', \cdots, t_n'\}\, t_j'\left(x_j, y_j, z_j\right)_{j=1,2,\cdots,n} \end{cases} \quad (6)$$

Step 4: After obtaining the corresponding points, the optimal rotation and translation matrix are obtained by the least squares method. The space conversion parameters $R_{accurate}$ and $T_{accurate}$ are calculated between the nearest corresponding point pairs s_i'' and t_j'.

Step 5: The rotation matrix $R_{accurate}$ and the translation vector $T_{accurate}$ are applied to the source point cloud S'' to obtain a new nearest point-to-point set S''', as shown in Equation (7).

$$S''' = \{s_1''', s_2''', s_3''', \cdots, s_n'''\}\, s_i'''\left(x_i, y_i, z_i\right)_{i=1,2,\cdots,n} \quad (7)$$

The mean of Euclidean distance D is calculated between the two point sets S''' and T', as shown in Equation (8).

$$D = \frac{\sum_{i=1}^{n} \sqrt{\left[s_i'''(xi) - t_i'(xi)\right]^2 + \left[s_i'''(yi) - t_i'(yi)\right]^2 + \left[s_i'''(zi) - t_i'(zi)\right]^2}}{n} \quad (8)$$

If $D \le \tau$ (τ is a given distance threshold), the process ends; otherwise, the above steps are repeated until the convergence conditions are met (as shown in Figure 4).

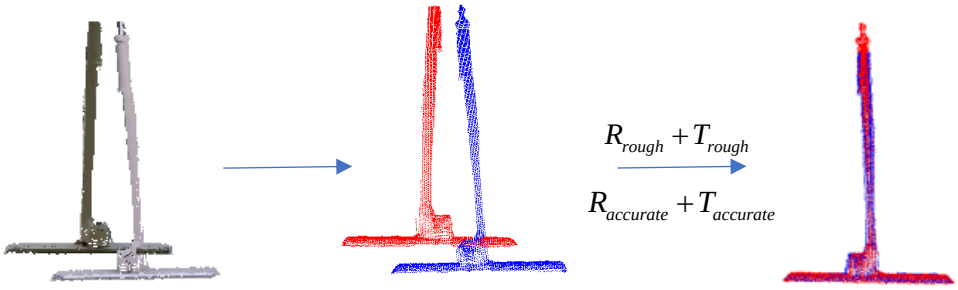

Fig. 4 - Calibration point cloud registration process

The left and right point clouds are rendered in red and blue respectively, according to the rough registration transformation parameters R_{rough} and T_{rough}, as well as the fine registration transformation parameters $R_{accurate}$ and $T_{accurate}$. The left and right point clouds are rendered into red and blue respectively, and the left pig point cloud is spatially transformed to complete the pig point cloud registration (as shown in Figure 5).

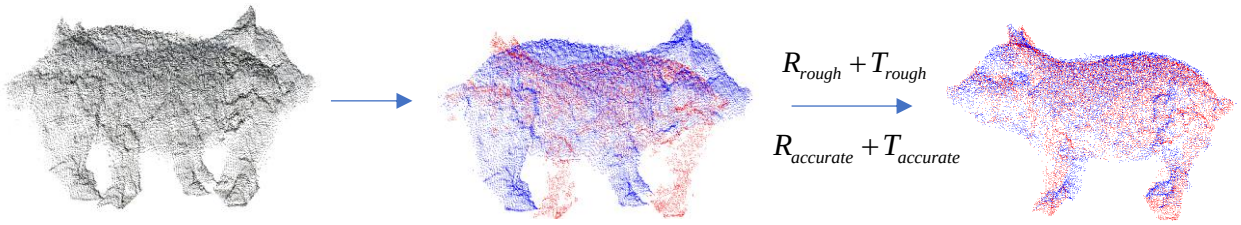

Fig. 5 - Pig point cloud registration process

Coordinate system correction based on plane normal vector

When Kinect v2 acquires the point cloud, it creates a coordinate system with the camera position as the origin. In order to facilitate the measurement of the pig point cloud, the origin of the coordinate system needs to be adjusted to the centre of the point cloud, and make the coordinate system X-axis register with the body width direction, Y-axis register with the body length direction, and Z-axis register with the body height direction.

Firstly, the ground normal vector n_z is used as the Z-axis of the new coordinate system. Then the maximum cross-section of the point cloud along the body length direction is found, and its normal vector n_x as the X-axis of the new coordinate system. The n_y of the new coordinate system is obtained by taking the cross product of n_z and n_x. Finally, the coordinate system is established with the centre of the point cloud as the coordinate origin (as shown in Figure 6).

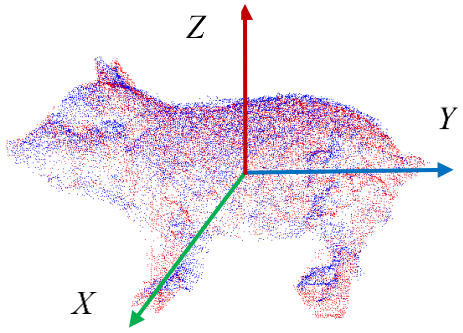

Fig. 6 - Coordinate system correction

Pig body measurement

Body length

The body length of the pig is defined as the length along the curve of its back from the midpoint of each ear to the base of the tail. Only the upper half of the pig's point cloud is needed, so $Z \geq 0$ part is selected. In order to extract the back curve of the pig, the point cloud of the pig was sliced in the range of $-0.01 \leq X \leq 0.01$.

A polynomial fit was applied to the dorsal curve and all extreme points and points of maximum curvature of the curve were calculated. The first extreme point is chosen as the starting point and the point of maximum curvature as the end point, and the length of the curve between these two points is calculated as the body length of the pig. The specific process is shown in figure 7.

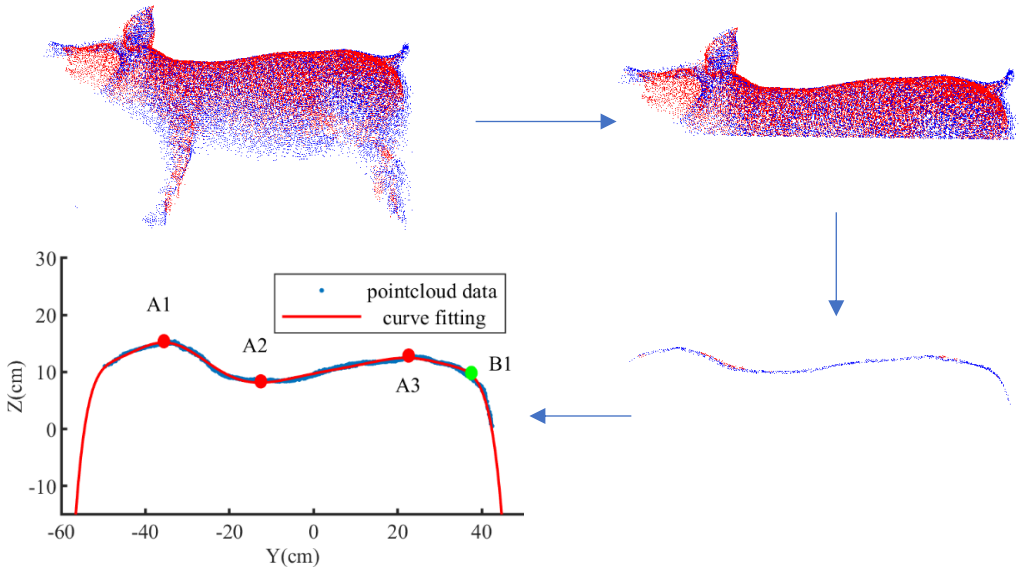

Fig. 7 - Schematic diagram of body length measurement

Body width

The body width is defined as the distance between the widest points of the abdomen. However, the width of the forelimbs and hindlimbs can affect this measurement of body width. To exclude this effect, the point cloud was divided into eight equal parts along the Y-axis direction, and the two parts near the origin were taken.

The difference between the maximum and minimum values of this part in the X-axis direction was calculated as the pig body width. The process is shown in figure 8.

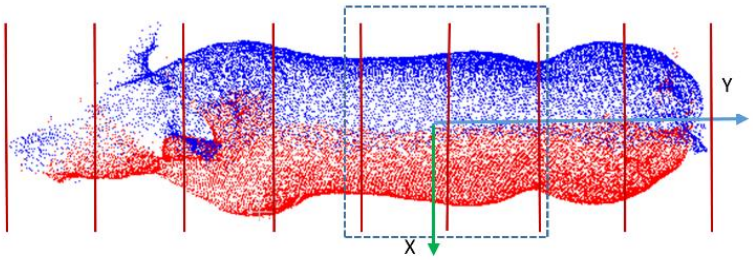

Fig. 8 - Schematic diagram of body width measurement

Body height

The body height of the pig is defined as the distance from the highest point of its back to the ground, which is the same as the body width measurement. However, the head can affect the body height measurement. In order to exclude this effect, the point cloud needs to be divided into eight equal parts along the Y-axis.

The four parts near the origin are selected, and the difference between the maximum and minimum values of the Z-axis is then calculated as the body height of the pig. The process is shown in figure 9.

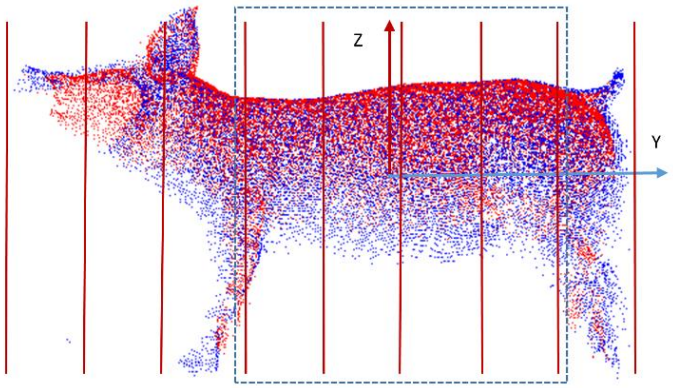

Fig. 9 - Schematic diagram of body height measurement

Abdominal circumference

The abdominal circumference of a pig is defined as the body circumference at the widest point of its abdomen. However, due to the horizontal camera angle, the pig's abdomen may not be fully captured. To compensate for this, the curve needs to be filled in using ellipse fitting, based on a plane perpendicular to the Y-axis and determined by two body width measurement points.

The fitted ellipse circumference was used as the abdominal circumference. The process is shown in figure 10.

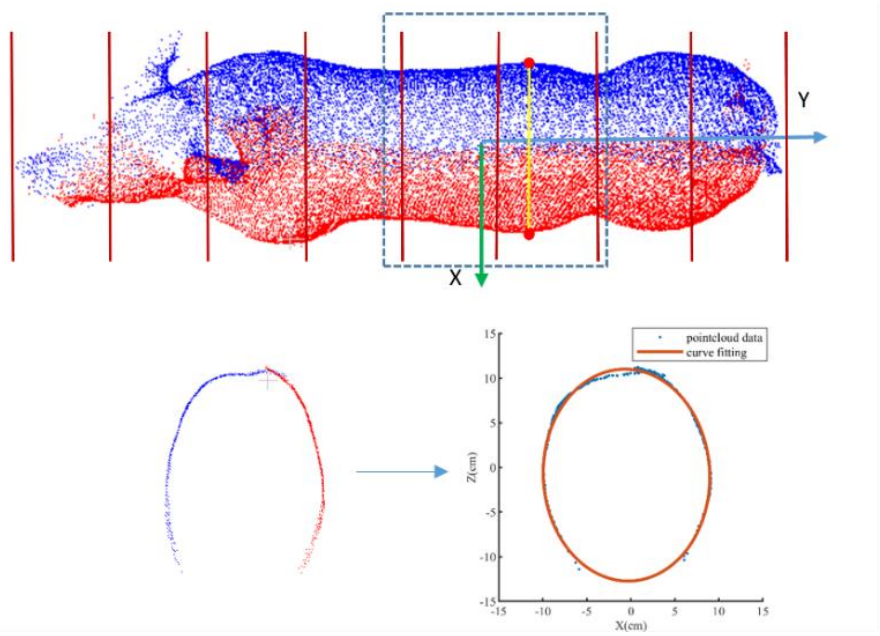

Fig. 10 - Schematic diagram of body Abdominal circumference measurement

RESULTS

In order to verify the accuracy of the algorithm for pig body size detection, a model of 100 pigs was used to register and measure the body size parameters in the experiment. To visually compare the manual and automatic measurements, a comparison graph was created for 20 randomly selected pigs, as shown in Figure 11. The MAPEs of body length, body width, body height and abdominal circumference were found to be 2.13%, 1.02%, 1.05% and 2.21%, respectively, which indicates that the proposed algorithm shows a significant degree of robustness accuracy.

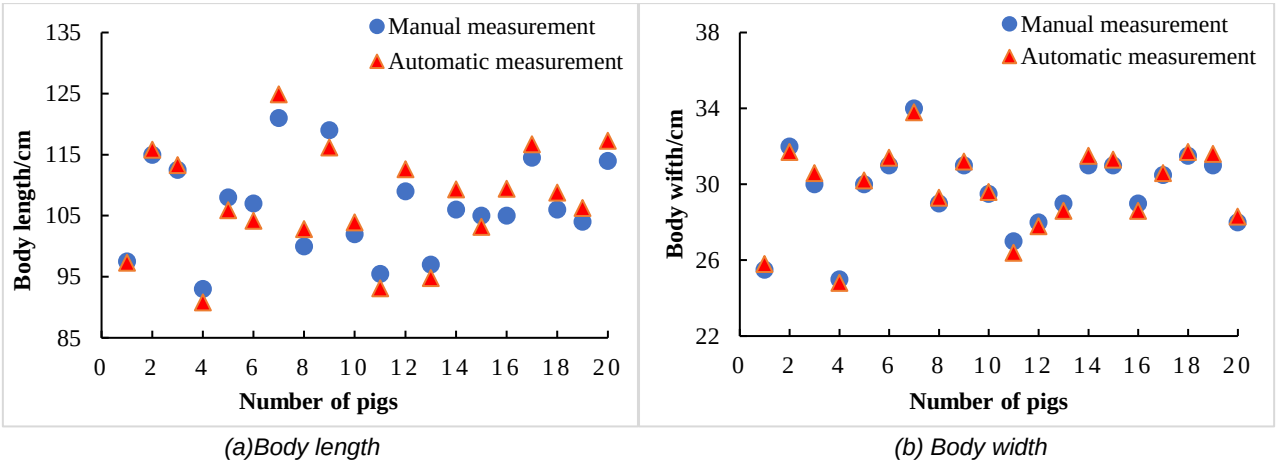

(a)Body length *(b) Body width*

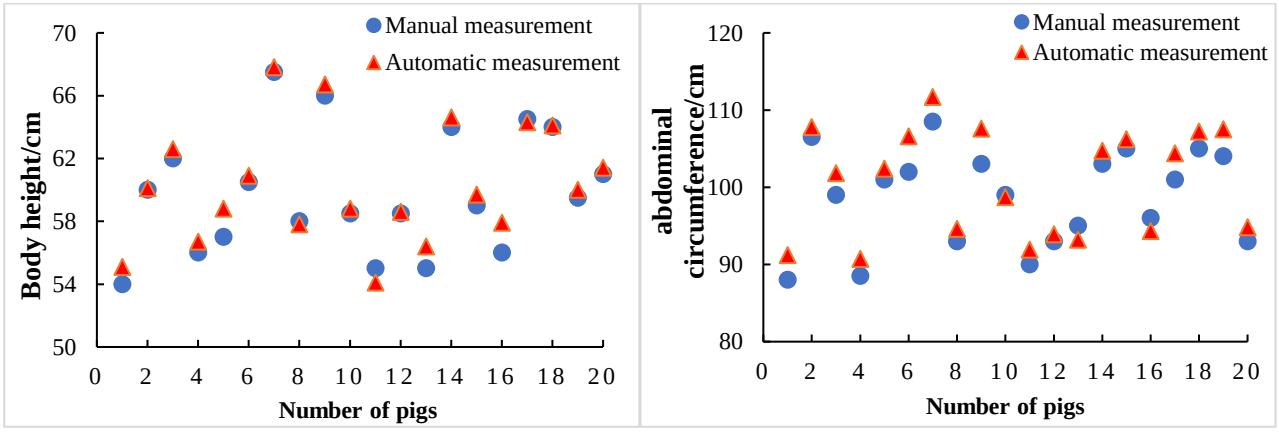

(c)Body height *(d)Body abdominal circumference*

Fig. 11 - Comparison chart of manual measurement and automatic measurement

CONCLUSIONS

In this paper, a curve-fitting-based method was proposed for accurately measuring the body size of pigs through point cloud processing and curve fitting. The method was validated in a measurement experiment involving 20 pigs, which demonstrated high accuracy. However, it is obvious that the MAPE of body width and height is smaller than that of body length and abdominal circumference. During system measurement, body height and body width were directly calculated as the straight-line distance between two points. In contrast, body length and abdominal circumference required curve fitting before their length could be calculated. This curve fitting process increased the potential for error between the actual and measured values. Furthermore, the measurement requires the pig to be in a strict upright posture without bending its body, which limits the system's practical application. Further research should aim to reduce the influence of posture on measurement results and improve the system's practical relevance.

ACKNOWLEDGEMENT

This study was supported by Key R&D program of Hebei Province(20326620D) and National key research and development program (2021YFC0122704).

REFERENCES

[1] Apirachai W., Banchar A., Supachai P., (2015). An approach based on digital image analysis to estimate the live weights of pigs in farm environments. *Computers and Electronics in Agriculture*, Vol.115, pp.26-33, Khon Kaen/ Thailand.

[2] Bewley J.M., Peacock A.M., Lewis O., (2008). Potential for estimation of body condition scores in dairy cattle from digital images. *Journal of dairy science*, Vol.94, Issue 9, pp.3439-3453, West Lafayette/UK.

[3] Chen C., Liu T., Wu W., (2018). Application and development of three-dimensional sensor Kinect in agriculture. *Jiangsu Agricultural Sciences*, Vol.46, Issue 8, pp.11-14, Yangzhou/China.

[4] Cheng H.J., Wang L., (2021). The impact of animal welfare on breeding efficiency. *Journal of Zhejiang Agricultural Sciences*, Vol.62, Issue 10, pp.2084-2086+2090, Zhejiang/China.

[5] Guo H., Ma X., Ma Q., (2017). LSSA_CAU: An interactive 3d point clouds analysis software for body measurement of livestock with similar forms of cows or pigs. *Computers and Electronics in Agriculture*, Vol.138, pp.60-68, Beijing/China.

[6] He X.Y., Zhao S.L., Zhang Z., Zhao T.Y., (2020). Development Trend of the Research and Application of Machine Vision. *Machinery Design & Manufacture*, Issue 10, pp. 281-283+287, Shenyang/China.

[7] Junming H., Hongjie Z., Li J., Yao E., & Weixue H. (2020). Analysis and optimization on the process of adjustable double drum castor shelling based on discrete element method. *INMATEH-Agricultural Engineering, (3).*

[8] Li Z., Du X.D., Mao T.Y., (2018). Pig body size detection system based on depth image. *Swine Industry Outlook*, Issue 4, pp.26-33, Beijing/China.

[9] Liu M.J., (2020). Infection mechanism and epidemic prevention measures of swine disease. *Animal Husbandry and Veterinary Medicine Today*, Vol.36, Issue 3, pp.22, Hunan/China.

[10] Liu T.H., Teng G.H., Zhang S.N., (2014). Reconstruction and application of 3D pig body model based on point cloud data. *Transactions of the Chinese Society for Agricultural Machinery*, Vol.45, Issue 6, pp.291-295, Beijing/China.

[11] Luo W.X., Luo F., Guo Y.J., (2018). Talking about the matters needing attention in the daily work of measuring pigs in the centre. *Northern Animal Husbandry*, Issue 10, pp.19, Hebei/China.

[12] Pezzuolo A., Guarino M., Sartori L., (2018). On-barn pig weight estimation based on body measurements by a Kinect v1 depth camera. *Computers and Electronics in Agriculture*, Vol.148, pp.29-36, Veneto/ Italy.

[13] Reinke N.A., Bogner M., (2021). Non-Contact Measurement for Resource-Efficient Production. *IST International Surface Technology*, Vol.14, Issue 1, pp.48-49, Winterthur/ Schweiz.

[14] Salau J., Haas J.H., Junge W., (2014). Feasibility of automated body trait determination using the SR4K time-of-flight camera in cow barns. *Springer Plus*, Vol.3, Issue 1, pp.1-16, Kiel/Germany.

[15] Viazzi S., Bahr C., Van H.T., (2014). Comparison of a three-dimensional and two-dimensional camera system for automated measurement of back posture in dairy cows. *Computers and Electronics in Agriculture*, Vol.100, pp.139-147, Leuven/Belgium.

[16] Wang D.F., Huang H.N., Zhang H.J., (2018). Current situation and development analysis of engineering technology research on pig breeding facilities. *Transactions of the Chinese Society for Agricultural Machinery*, Vol.49, Issue 11, pp.8-21, Harbin/China.
[17] Wang K., Guo H., Ma Q., (2018). Pig body size measurement method based on mirror reflection of single angle point cloud. *Transactions of the Chinese Society for Agricultural Machinery*, Vol.49, Issue 3, pp.187-195, Beijing/China.
[18] Weber A., Salau J., Haas J.H., (2014). Estimation of backfat thickness using extracted traits from an automatic 3D optical system in lactating Holstein-Friesian cows. *Livestock Science*, Vol.165, Issue 1, pp.129-137, Kiel/Germany.
[19] White R., Schofield C., Green D., Parsons D., Whittemore C., (2004). The effectiveness of a visual image analysis (VIA) system for monitoring the performance of growing/finishing pigs. *Animal Science*, Vol.78, Issue 3, pp.409-418, Bedford/UK.
[20] Yin L., Cai G.Y., Tian X.H., (2019). Three dimensional point cloud reconstruction and body size measurement of pigs based on multi-view depth camera. *Transactions of the Chinese Society of Agricultural Engineering*, Vol.35, Issue 23, pp.201-208, Guangzhou/China.
[21] Zhang L.L., (2021). The impact of African swine fever on my country's pig breeding industry. *Animal Husbandry and Veterinary Science (Electronic Edition)*, Issue 3, pp.158-159, Jilin/China.